

EFFECT OF REACTION TIME ON STRUCTURAL AND OPTICAL PROPERTIES OF POROUS SiO₂ NANOPARTICLES

E. A. G. ENSKU ALI^{a,b}, K. A. MATORI^{a,c*}, E. SAION^c, H. A. A. SIDEK^c,
M. H. M. ZAID^{a,c}, I. M. ALIBE^{a,d}

^a*Materials Synthesis and Characterization Laboratory, Institute of Advanced Technology, Universiti Putra Malaysia, 43400 UPM Serdang, Selangor, Malaysia.*

^b*School of Fundamental Sciences, Universiti Malaysia Terengganu, 21030 Kuala Terengganu, Terengganu, Malaysia.*

^c*Department of Physics, Faculty of Science, Universiti Putra Malaysia, 43400 UPM Serdang, Selangor, Malaysia.*

^d*National Research Institute for Chemical Technology Zaria, Kaduna State Nigeria*

The effect of different reaction time on the structural and optical properties of porous SiO₂ nanoparticles by simple precipitation method was comprehensively studied in this work. In this study, an aqueous sodium silicate was reacted with ethanol in deionized water and stirred between 30 to 180 min as for mixture to react. The filtered product was subjected to drying and characterized by X-ray diffraction (XRD), transmission electron microscopy (TEM), Fourier transform infrared reflection (FTIR), surface area analyzer, Raman and UV-Vis spectroscopy. The produced SiO₂ nanoparticles powder was in amorphous form with the average particle size less than 100 nm. The sample with reaction time 90 min shows fine porous characteristic with the highest specific surface area and average pore volume. This different characteristic also gives a significant change in optical properties of the final product.

(Received January 23, 2017; Accepted May 22, 2017)

Keywords: Porous silica, Raman measurement, Optical properties, Simple precipitation method, Amorphous silica

1. Introduction

Silica (SiO₂) is one of the materials used in various applications according to the targeted application due to its excellent physicochemical, mechanical and optical properties especially in displays and lighting devices [1]. The research on the performance of the SiO₂ mainly depends on its density, size, surface area, and structural properties. Nowadays, nanosize particles with porous and hollow inner core structure has attracted considerable interest due to the advantage during synthesis and utilization in medical (drug delivery) [2], catalysis [3] and electro-optical [4,5]. Mostly, SiO₂ nanoparticles were synthesized by sol-gel, reverse microemulsion and flame synthesis method [6] involving hydrolysis and condensation reaction of metal alkoxide (Si(OR)₄) such as tetraethyleorthosilicate (TEOS) or inorganic salt such as sodium silicate in the presence of acid or base as catalyst. The combination of silicon tetraacetate with poly(vinyl pyrrolidone) (PVP) as capping agent to produced SiO₂ nanoparticles by simple heat treatment method was reported by Alibe [7]. The use of TEOS and silicon tetraacetate as a silica precursor can give some drawback due to its toxicity and relatively expensive [8]. For that reason, sodium silicate or water glass was among the choices as to produce SiO₂ porous nanoparticles. The availability, low in cost and toxicity during the handling process has given it an advantage. Moreover, the source sodium

*Corresponding author: khamirul@upm.edu.my

silicate also can be from industrial or agricultural waste materials for example from coal fly ash [9] and rice husk [10,11].

The synthesis of SiO₂ porous nanoparticles usually involving the use of surfactant along with catalyst agent of acid or base and by several methods such as sol-gel, co-precipitation, hydrothermal [12,13]. Alongside with the cheaper precursor, the application of simple synthesis process can give benefit in term of production cost.

In this work, a simple precipitation process was chosen to produce porous SiO₂. The aqueous sodium silicate was used as a silica source and reacted with ethanol without using of templates or surfactant. The effect of reaction or stirring time after the mixing of both precursors was studied by X-ray diffraction (XRD), transmission electron microscopy (TEM), Fourier transform infrared reflection (FTIR) spectroscopy, surface area analyzer and Raman spectroscopy.

2. Experimental

2.1 Synthesis of silica nanopowder

The synthesis of silica nano powder was based on the modification of simple precipitation method for silicate preparation [14, 15]. Firstly, 10 ml of sodium silicate solution (> 27% SiO₂) from Sigma Aldrich was mixed with 300 ml of deionized water. Then, 90 ml of ethanol (95%) from System was added to the mixture and sudden reaction formed semi transparent white suspension. The resulting mixture was stirred with magnetic stirrer at speed of 500 rpm in room temperature for reaction time from 30 to 180 min. At the end of reaction time, the suspension was filtered with membrane filter connected to vacuum pump and washed with deionized water for several times in order to rinse the remaining by products. The wet suspension was put to drying in oven at 90 °C for 24 hours.

2.2 Characterizations

To study the structural characteristic of synthesized SiO₂ nanopowder, the sample was characterized by XRD (PANalytical X'pert PRO PW 3040 MPD), TEM (Hitachi H-7100) and FTIR spectrometer (Perkin Elmer Spectrum 100). In addition, the optical property was characterized using UV-Visible (Shimadzu UV-3600) spectrometer for optical absorption and band gap determination. Surface area analysis by nitrogen gas adsorption and desorption studies were carried out on a Belsorp Mini II operated at 250 °C for 3 hr and Raman spectroscopy (Witec Alpha 300R) at 532.14 nm excitation wavelength.

3. Results and discussion

Porous SiO₂ nanoparticles were produced by simple co-precipitation reaction of aqueous sodium silicate and ethanol. The samples denoted as S1, S2, S3, S4 and S5 for reaction time of 30, 60, 90, 120, and 180 min respectively. Fig. 1 shows XRD diffractogram of SiO₂ nanoparticles that reveals all of sample are amorphous. The infrared spectroscopy in Fig. 2 shows the significant peak at 1072 cm⁻¹ corresponds to asymmetric vibration of the siloxane bond, Si-O-Si [11] and it has no significant difference with other samples. The peak located at 957, 797 and 448 cm⁻¹ are assigned to Si-OH asymmetric bending vibration, Si-O symmetric stretching vibration and bending vibration [16]. The presence of absorption at 3408 and 1638 cm⁻¹ belonged to -OH stretching vibration of the silanols or adsorbed water molecules on the surface. The silica characteristic clearly can be seen in S3 sample by vibrational peak at 1072, 957, 797 and 448 cm⁻¹ that are assigned to asymmetric stretching of Si-O-Si, symmetric stretching of SiO₄, torsional vibration modes of SiO₂ and asymmetric deformation of SiO₄ respectively [17,18,19,20]. The asymmetric stretching of Si-O-Si also reported as a surface silanol group bending peak [21] because of the availability of hydroxyl due to drying at 90 °C.

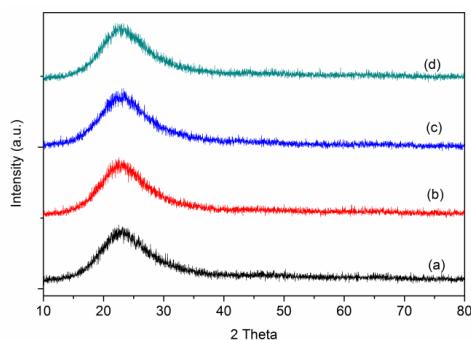


Fig. 1. XRD diffractogram of (a) S1, (b) S2, (c) S3 and (d) S4

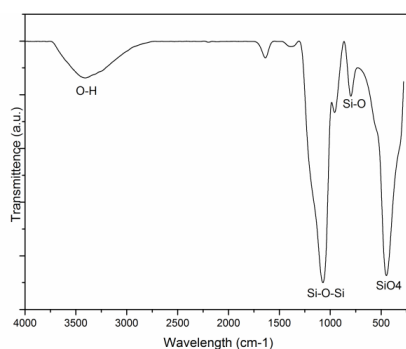


Fig. 2. FT-IR spectrum for S4

Fig.3 shows TEM image of the spherical shape of nanoparticles with the average radius gradually increased between 75.41 to 99.03 nm with increase of reaction time. Agglomerations of particles start to form at 120 min stirring time. Although the outer layer looks like the same, the transparent like a blotch within the spherical nanoparticles was observed due to the less in density of the inner core shell. From the N_2 adsorption and desorption isotherm and the pore size analysis, the average pore size was higher for samples synthesis for sample with 30, 60 and 90 min reaction time (Table 1) with the highest at 90 min. The samples with reaction time 30 and 90 min exhibit a type III isotherm according to IUPAC classification [22,23] that referring to weak gas-solid interaction basically for nonporous or microporous materials. In accordance with this result, it supports the existence of porosity within the spherical nanoparticles as in TEM images. The high absorption at the relatively $p/p_0 > 0.8$ point out that nitrogen gas was blocked from infiltrating the inner shell structure at lower pressure because of the dense outer layer. For the samples reacted at 120 and 180 min, the dense particles which reduced in pore within the core shell was observed. From the Brunauer-Emmett-Teller (BET) specific surface analysis, the values decreased from 34.149 to 21.570 m^2g^{-1} with reaction time (Table 1) because of the increased of particles size and agglomeration at higher reaction time of the nanoparticles.

The reaction of SiO_2 nano particles produced by reacting aqueous sodium silicate with ethanol is basically the hydrolysis and condensation reaction. When sodium silicate was diluted in deionized water, hydrolysis reaction formed $Si(OH)_4$ and sodium ions. When added to ethanol, the forming of semi transparent white suspension indicates the grown of silicate particles. The washing of solid precipitated during vacuum infiltration has extracted the unsolidified silicate anions due to its high solubility in water [15]. This gives the porous like structures depending on the reaction time and for longer time, the dense particle was observed.

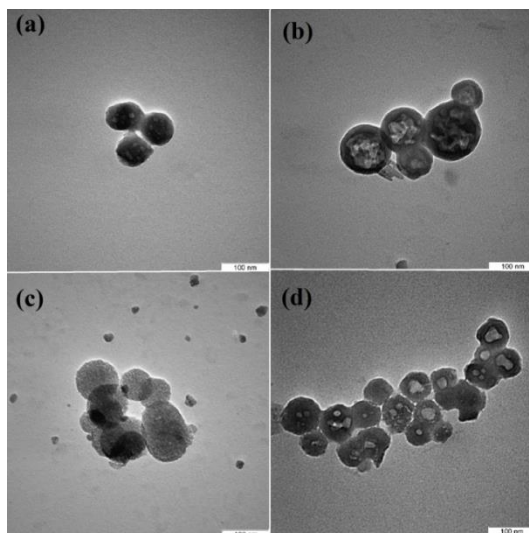


Fig. 3. TEM image for (a) S1, (b) S2, (c) S3 and (d) S4

Table 1 Effect of reaction time to the BET specific surface area and pore properties

Sample	Average diameter (nm)	BET specific surface area ($\text{m}^2 \text{g}^{-1}$)	Total pore volume ($\text{cm}^3 \text{g}^{-1}$)	Average pore diameter (nm)
S1	75.41	34.149	0.4011	52.80
S2	86.51	29.310	0.4508	54.75
S3	86.73	29.308	0.4804	54.73
S4	91.33	22.715	0.0293	5.15
S5	99.03	21.570	0.0264	3.35

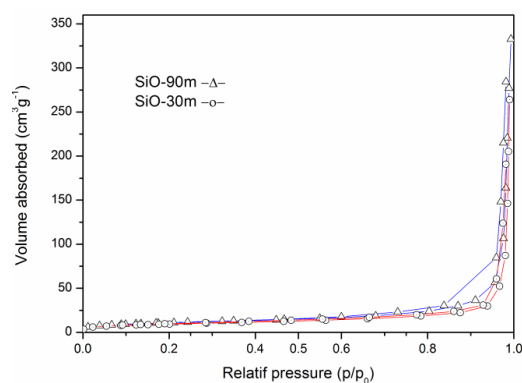


Fig. 4. Nitrogen gas adsorption/desorption isotherm of SiO_2 nanoparticles for 30 and 90 min reaction time

The effect of reaction time can be further evaluated by Raman spectra. In Fig.5, the intensity of the band between 350 to 500 cm^{-1} wavelength was observed. In this range of wavelength, the number of membered Si-O ring can affect the band peak characteristic. The breathing mode of 4-membered rings, known as D1 line ($\sim 490 \text{ cm}^{-1}$) was low in intensity for S1, S2 and S3. The lowering of this band was related to the observation of the larger pores [24].

The R-band ($\sim 440\text{cm}^{-1}$) that associated with Si-O-Si oxygen vibration or oxygen bond angle, exhibit the increased of peak band for S4 and S5 sample. It seems possible that these results are due to the higher mean intertetrahedral bond angle compared to S1, S2 and S3 sample. This finding support the formation of smaller rings that could attributed to smaller particles size. This results agrees with the findings of another study in which the Raman spectra can be use to differentiate the structure or properties of the core and surface shell of SiO_2 nanoparticles [25]. The effect of reaction time to the structural relaxation for the R-band shift is certainly due to the different structure of SiO_2 nanoparticles inner core as shown in TEM and pore properties. The shift of R-band shows that the shell surface characteristic is dominant in the spectra revealing the lowering of membered rings, thus lowering Si-O-Si angle [26].

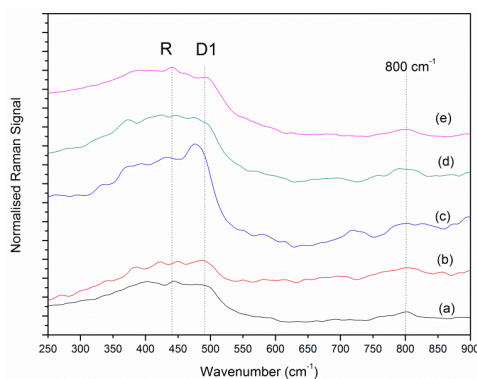


Fig. 5 Raman spectra (range $200\text{-}900\text{ cm}^{-1}$) for (a) S1, (b) S2, (c) S3, (d) S4 and (e) S5

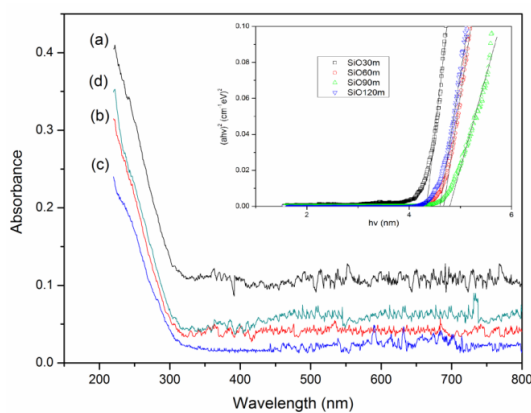


Fig. 6 UV-Vis absorbance spectra for (a) S1, (b) S2, (c) S3, (d) S4 and band gap calculation (inset)

Optical properties likewise FT-IR and Raman spectra, UV-Vis are usually sensitive to any nanocrystal surface. Fig 6 shows UV-Vis spectrum of amorphous silica nanoparticles with different reaction time. The strong absorption edge is observed at 300 nm wavelength. The optical band gap was determined from absorption coefficient value. The relation is given by equation (1)

$$(\propto hv)^2 = A(hv - E_g) \quad (1)$$

With A as a constant, the photon energy is denoted by hv and E_g is the optical energy band [27]. Fig.6 is the plot of $(\propto hv)^2$ versus hv and values of linear region from individual plot lines to x -axis intercept will give optical band gap value. The band gaps were 4.34, 4.61, 4.75 and 4.68 eV for sample S1, S2, S3, and S4 respectively. The sample with reaction 90 min reaction time

gives the highest band gap. This can be related to the porosity characteristic exhibit by this sample as depicted in Raman and surface area analysis.

4. Conclusions

An amorphous SiO₂ nanoparticles was successfully synthesis by precipitation reaction of sodium silicate with ethanol. The XRD diffractogram and IR spectra shows the amorphous phase and the formation of Si-O bond.

The porosity and surface area of nanoparticles depends on the reaction time after mixing with the highest porosity at 90 min reaction time and denser particles produced with longer reaction time. The particular properties of the inner core of particle revealed in Raman spectra, shows the dominant characteristic of porous SiO₂ nanoparticles.

Acknowledgments

The authors gratefully acknowledged the financial support for this study from the Malaysian Ministry of Higher Education (MOHE), Universiti Malaysia Terengganu and Universiti Putra Malaysia through the Fundamental Research Grant Scheme (FRGS) and Inisiatif Putra Berkumpulan (IPB) research grant.

References

- [1] K. J. Klabunde, *Nanoscale Materials in Chemistry*, Wiley-Interscience, USA, 2001.
- [2] A. M. El-Toni, A. Khan, M. A. Ibrahim, M. Al-Hoshan, J. P. Labis, *Molecules* **17**, 13199 (2012).
- [3] X. Du, J. He, *Nanoscale* **3**, 3984 (2011).
- [4] K. Sowri Babu, A. Ramachandra Reddy, C. Sujatha, K. Venugopal Reddy, *Ceram. Int.* **39**, 3055 (2013).
- [5] Q.-L. Ma, B. -G. Zhai, Y. M. Huang, *J. Sol-Gel Sci. Techn.* **64**, 110 (2012).
- [6] I. A. Rahman, V. Padavettan, *J. Nanomater.* **2012**, 1 (2012).
- [7] I. M. Alibe, K.A. Matori, E. Saion, A.M. Alibe, M.H.M. Zaid, E.A.A. Ghapur Engku, *Dig. J. Nanomater. Bios.* **11**, 1155 (2016).
- [8] N. Baccile, F. Babonneau, B. Thomas, T. Coradin, *J. Mater. Chem.* **19**, 8537 (2009).
- [9] M. Halina, S. Ramesh, M.A. Yarmo, R.A. Kamarudin, *Mater. Chem. Phys.* **101**, 344 (2007).
- [10] T. Liou, C. Yang, *Mater. Sci. Eng. B.* **176**, 521 (2011).
- [11] F. Adam, T.-S. Chew, J. Andas, *J. Sol-Gel Sci. Techn.* **59**, 580 (2011).
- [12] N. A. Rahman, I. Widhiana, S. R. Juliastuti, H. Setyawan, *Colloids and Surfaces A* **476**, 1 (2015).
- [13] T. Jesionowski, *J. Mater. Process. Tech.* **203**, 121 (2008).
- [14] R. H. M. Godoi, L. Fernandes, M. Jafellici Jr, R. C. Marques, L. C. Varanda, M. R. Davolos, *J. Non-Cryst. Solids* **247**, 141 (1999).
- [15] C. Y. Jung, J. S. Kim, T. S. Chang, S. T. Kim, H. J. Lim, S. M. Koo, *Langmuir* **26**, 5456(2010).
- [16] N. S. C. Zulkifli, I. Ab Rahman, D. Mohamad, A. Husein, *Ceram. Int.* **39**, 4559 (2013).
- [17] A. M. Ali, A. A. Ismail, R. Najmy, A. Al-Hajry, *J. Photoch. Photobio.* **A275**, 37 (2014).
- [18] V. M. Gun'ko, V.M. Bogatyrov, O. I. Oranska, L.I. Borysenko, J. Skubiszewska-Zięba, A. Książek, R. Leboda, *Appl. Surf. Sci.* **276**, 802 (2013).
- [19] Q. Lu, P. Wang, J. Li, *Mater. Res. Bull.* **46**, 791 (2011).
- [20] K. Sowri Babu, A. Ramachandra Reddy, C. Sujatha, K. Venugopal Reddy, *Ceram. Int.* **39**, 3055 (2013).
- [21] I. A. Rahman, P. Vejayakumaran, C. S. Sipaut, J. Ismail, C.K. Chee, *Mater. Chem. Phys.* **114**, 328 (2009).

- [22] J. Cui, H. Sun, Z. Luo, J. Sun, Z. Wen, *Mater. Lett.* **156**, 42 (2015).
- [23] A. Ganguly, T. Ahmad, A.K. Ganguli, *Langmuir* **26**, 14901 (2010).
- [24] C. Kinowski, M. Bouazaoui, R. Bechara, L.L. Hench, J.M. Nedelec, S. Turrell, *J. Non-Cryst. Solids* **291**, 143 (2001).
- [25] A. Alessi, S. Agnello, G. Buscarino, F.M. Gelardi, *J. Raman Spectrosc.* **44**, 810 (2013).
- [26] G. Vaccaro, S. Agnello, G. Buscarino, M. Cannas, L. Vaccaro, *J. Non-Cryst. Solids* **357**, 1941 (2011).
- [27] B. D. Viezbicke, S. Patel, B. E. Davis, D. P. Birnie, *Phys. Status Solidi*, **11**, 2015.